# Preliminary Analysis of Network Fragility and Resilience in Large Electric Grids

Adam B. Birchfield
Department of Electrical and Computer Engineering
Texas A&M University
College Station, Texas
abirchfield@tamu.edu

Jayant Patil, Roger Paredes, Leonardo Dueñas-Osorio
Department of Civil and Environmental Engineering
Rice University
Houston, Texas
jayant.patil@rice.edu, roger.paredes@rice.edu,
leonardo.duenas-osorio@rice.edu

***Abstract*—This paper introduces and compares two frameworks for evaluating and quantifying the network fragility and resilience of large, high-voltage transmission grids, with example applications given for validating synthetic test case datasets. The first framework uses an all-terminal reliability metric based on graph-theoretic probabilistic connectivity analysis, allowing for a more precise determination of the distribution and edge cases of fragility. The other network resilience framework considered here analyzes maximal load delivery capability, as evaluated by a linearized optimal power flow analysis that allows load shedding. This analysis is performed under multiple component outage conditions, along the full spectrum from ordinary operation to complete non-availability of the extra-high voltage grid. The range of results indicates grid performance under three types of outage sets: planned outages, random outages, and targeted outages. Example results for the North-Central area of the 2000-bus synthetic Texas test case show the application of the two methods.**

***Keywords*—Electric grid resilience, grid reliability, cascading failure, synthetic electric grids**

## I. Introduction

The purpose of fragility and resilience analysis for electric transmission grids is to explore the performance of these systems to a variety of disturbances, particularly due to extreme, high-impact events. The goal is to assess, under adverse events of varying magnitudes, to what degree this critical energy delivery infrastructure can continue its functionality, and how quickly it can be restored to full operation. Previous work in the area of power system resilience has stressed the importance of examining the whole life cycle of an event, from preparedness to degradation during the event to short-term and long-term restoration [1]. High-impact scenarios of interest include natural disasters [2]-[4], electromagnetic events natural or manmade [5], and cyber-physical events [6]. The recent controlled outages in Texas due to extreme winter weather are an example that highlight the severe negative impact that rare events can have. A key aspect of fragility and resilience quantification is to look at the maximum load that can be served by a system at varying levels of network availability, either during system degradation or during restoration [4], [7]. There are many potential approaches to enhancing system resilience, such as network reconfiguration [8] and microgrid formation [9]-[10]. In the longer term, the design of the transmission network impacts how resilient the grid can be [8], [11].

This paper looks at the function of grid network structure on the ability of the electric grid to serve load at various levels of system degradation. To approach this problem, two parallel strategies are employed and compared. First, we use the all-terminal reliability (ATR) as a metric to compare different configurations of transmission line outages. As the number of possible outage configurations even in a mid-sized grid are combinatorically large, we use *principled approximation* sampling strategies in selecting outage configurations to evaluate the average and worst-case performance of the grid. Principled methods improve upon traditional sampling strategies which may miss rare-event, worst-case configurations thus overestimating the performance.

For a low number of transmission line failures, we use an enumeration strategy to evaluate the exact ATR with a full-factorial design of experiments. For higher number of line failures, where a full-factorial design of experiments becomes infeasible, we use a principled $(\epsilon, \delta)$-approximate sampling strategy which theoretically guarantees that the relative error of the approximation is less than the specified tolerance $\epsilon$ with at least $1-\delta$ confidence.

Second, an electric modeling-based approach is used to evaluate load service in degraded system conditions. That is, the analysis shows under potentially severe contingencies how much of the system demand can still be met with the remaining transmission and generation. This approach differs from a cascading failure analysis in that it assumes appropriate load shedding would be done, as necessary, to mitigate transmission system overloads and prevent a wider blackout. These scenarios have applications in preparing for a high-impact event, interpreting the scale of it, operating a degraded system, and prioritizing restoration activities.

The example used in this paper to demonstrate both methods starts with a synthetic power grid model with 8 areas and 2000 buses, geographically located on the state of Texas, but not modeling the actual Texas grid. Fig. 1 shows the grid's one-line diagram with areas color-coded. Prior work in building this and other synthetic grids has validated the realistic characteristics of these grids according to topological, geographic, and power flow characteristics [14]-[15]. Additional work has been done in making these grids reliable to N-1 security against expected ordinary events [16]. This grid also has generator cost curves and transient stability models in place [17]. The base case used in this analysis is freely available online [18].

The work for this paper was supported in part by funding from the U.S. Department of Energy's Advanced Research Project Agency-Energy (ARPA-E).

2021 IEEE Power and Energy Conference at Illinois (PECI) | 978-1-7281-8648-1/21/$31.00 ©2021 IEEE | DOI: 10.1109/PECI51586.2021.9435202

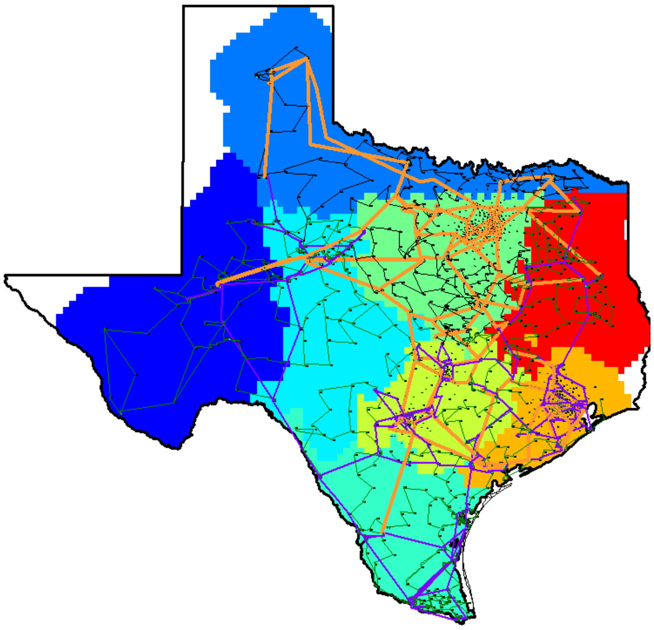

Figure 1. One-line diagram of the synthetic 2000-bus case, a fictitious, realistic grid geo-located in Texas, with areas color-coded. Orange lines are 500 kV, violet lines are 230 kV, lower voltage lines are shown in black and green.

## II. Fragility Modeling with All-Terminal Network Reliability

To identify the worst-case combinations of transmission line failures corresponding to the number of outages, we use the all-terminal reliability metric as the criterion. In the following subsections, we first define graph theory preliminaries and then the methodology used to evaluate ATR for increasing number of transmission line outages.

### *A. Graph theory preliminaries*

The underlying network model is an *undirected graph* $G = (\mathcal{V}, \mathcal{E})$, with a set $\mathcal{V}$ of vertices representing buses and a set $\mathcal{E}$ of edges representing branches. We let $\#\mathcal{V}$ and $\#\mathcal{E}$ be the number of vertices and edges, respectively. A graph $H$ is a *subgraph* of $G$, denoted by $H \subseteq G$, when the vertices and edges of $H$ are a subset of the vertices and edges of $G$. We say $G$ is *connected* if there are no subgraphs $H, H' \subseteq G$ such that the vertices (edges) of $H$ and $H'$ form a partition of the vertices (edges) of $G$. Also, $H_s \subseteq G$ is a *spanning* subgraph of $G$ if $H_s$ contains every vertex of $G$.

### *B. Availability under N-k outage scenarios*

For a graph $G$ with edge failure probabilities equal to $p$, the *all-terminal network reliability*, denoted $\mathrm{ATR}(G, p)$, is the probability that $G$ remains connected after every edge fails independently with probability $p$ [19]. For a given number of edge failures, the worst-case edge configurations are those that result in subgraphs with the smallest $\mathrm{ATR}(G, p)$.

For a given number of edge failures, $k$, and corresponding edge failure probability, $p_k$, the $N-k$ reliability analysis involves computing the $\mathrm{ATR}(G', p_k)$ of subgraph $G' = G - \{\mathcal{E}_k\}$, where $\{\mathcal{E}_k\}$ is a set of $k$ edges, for every possible $\{\mathcal{E}_k\}$. The $N-k$ reliability spectra is the distribution $\mathrm{ATR}(G', p_k)$ vs. $k$.

To compute the $\mathrm{ATR}(G', p_k)$, we use a Binary Decision Diagram (BDD) – based strategy proposed in [20]. To reduce the order of computations, as naïve enumeration is infeasible, reliability-preserving edge-contractions are performed on graph $G$ to give an equivalent graph $G^*$. As every graph $G'$ is a subgraph of $G$ (and equivalently $G^*$), we only need to construct the BDD corresponding to $G$ once, and assign the probability of failure corresponding to a particular edge outage as 1.0.

Similar to $N-k$ reliability analysis, we fix an outage-level ($k = 1, 2, \ldots$) and evaluate network availability $\mathrm{ATR}(H, p_k)$ for every possible outage scenario $H \in \mathcal{G}_k$ a connected spanning subgraph of $G$ with exactly $\#\mathcal{E} - k$ edges and $p_k$ the edge failure probability corresponding to the outage-level, $k$. For medium to large values of $\#\mathcal{E}$ and increasing values of $k$,

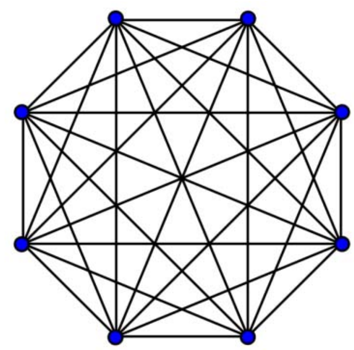

Figure 2. Complete graph with 8 nodes and 28 edges.

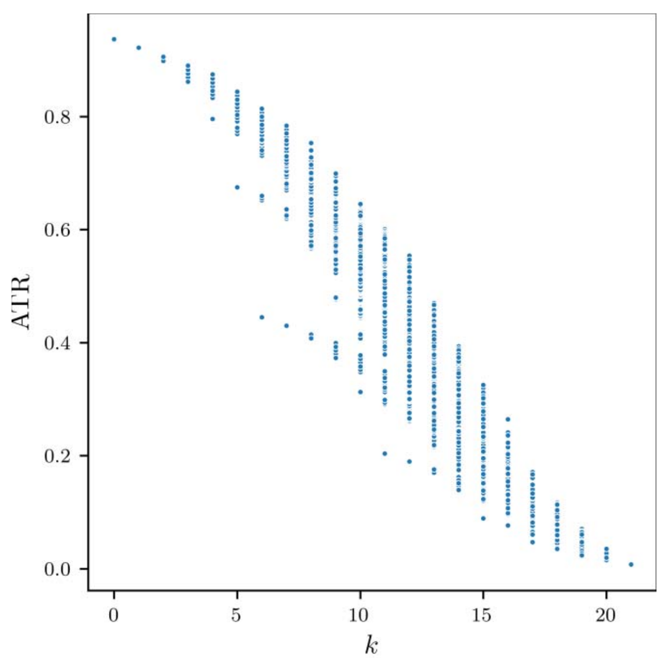


Figure 3. The $N-k$ full-spectra all-terminal reliability for the 8-node complete graph with 50% edge failure probability.

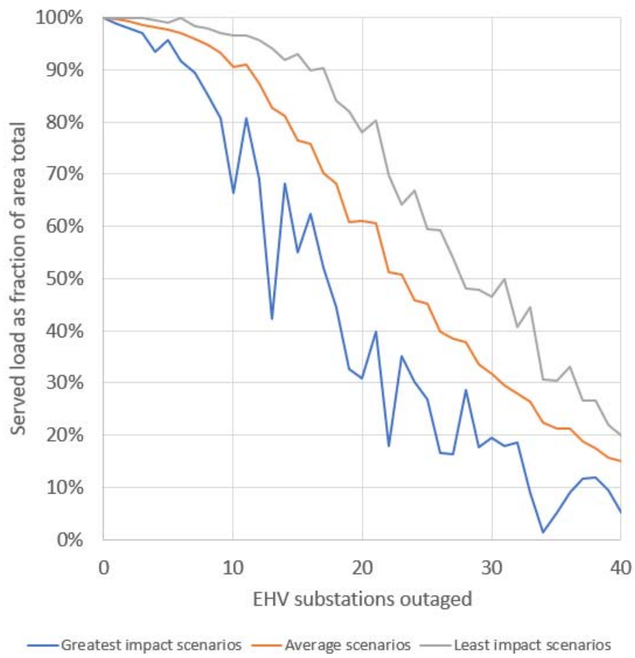


Figure 4. Maximum load delivery curve for north-central area (green in Fig. 1) under varying levels of substation outages.

the number of outage scenarios calculated as $\binom{\#\mathcal{E}}{k}$, can be combinatorically very large. Hence, we compute the exact distribution of availability for small $k$ and for larger values of $k$, we report the *mean* availability, i.e. $\overline{\mathrm{ATR}}(G,p,k) = (\#\mathcal{G}_k)^{-1} \sum_{H\in\mathcal{G}_k} \mathrm{ATR}(H,p)$. As an example, consider the 8-node complete graph, K8, as shown in Fig. 2. The $N-k$ full-spectra reliability distribution for the 8-node complete graph and with 50% edge failure probability is shown in Fig. 3.

For mean availability computations, we employ rigorous $(\epsilon,\delta)$-approximations (e.g. [21]), that are making inroads in reliability engineering [22]. For a quantity $q$ of interest and user-specified parameters $\epsilon,\delta \in (0,1)$, an $(\epsilon,\delta)$-approximation, $\tilde{q}$, guarantees that the relative error of $\tilde{q}$ is at most $\epsilon$ with at least confidence $1-\delta$. Alternatives to $(\epsilon,\delta)$-approximations, such as stopping rules based on the sample variance and approximate normal confidence intervals, are known to issue overconfident results (e.g. [23]). For our evaluations, we use the Gamma Bernoulli Approximation Scheme of [24].

## III. Fragility Modeling with Linearized Power Flow and Load Shedding

An actual, detailed study of the impact of any particular event would involve analyzing the sequence of events, transient dynamics, and assumptions about operational decisions. In order to more quickly summarize effects on larger numbers of scenarios, the modeling approach used in this section approximates all of these effects using a modified linearized (or "dc") optimal power flow (DCOPF). The DCOPF solves only for active power flows through a transmission network, optimizing the generator dispatch economically, subject to device limits, through solving a linear program. This approach is favored because of its quick and robust convergence and simplicity in focusing on the large-scale power delivery phenomena—more complex modeling might involve a diverging solution due to localized issues, not allowing a quantification of system availability. In this instance, load-shedding replaces true economic optimization. The assumption is that the transient phenomena are handled correctly by system controls and operator action, and there is enough time to utilize generator controls in order to correct overloads and serve as much load as possible. Voltage and reactive power phenomena are also not considered in this approach. In short, it preliminarily assumes best-case operations. The loads are considered control variables, assigned a constant linear cost associated with shedding them, with all actual generators set to zero cost. The system cost would therefore quantify minimal load shedding (along with all load outaged and islanded) and hence maximal load service.

Outages of extra-high voltage substations (EHV) and all the connected transmission lines are the main contingency considered here, as these represent a common and impactful mode of failure in extreme events and capture simultaneously the issues of transmission line stress and reduction of the availability of certain large generators. The approach here is to capture all levels of EHV substation outages for a given area, similar to N-k analysis. It is not computationally feasible to study all such combinations, as they grow factorially. Several approaches are examined in this paper to approximate this. One preliminary approach is uniform sampling, which for a smaller number of EHV substations in a single area (less than 60), will be expected to capture a large portion of the possible response spectrum. Additional methods involve logic-based and graph-theoretic methods to search for combinations likely to have more significant effects, such as presented in [12]-[13]. These studies are run for samples at each level of outage all the way from a single outage (N-1) through a complete outage of the entire EHV network, while guaranteeing uncertainty quantification in the process.

Here, the structural resilience analysis was performed for each of the 8 areas in the 2000-bus case. Fig. 4 summarizes the north-central area results, giving the range of observed load shedding required at various levels of EHV substation outages. It is clear that this particular area relies heavily on the EHV network, but can often withstand 10-20% of substation outages with only small amounts of load shedding necessary. Beyond 20%, the curve becomes much steeper, until with all the EHV gone only a small amount of load can be served by lower-voltage generators and imports along low-voltage ties to other areas. The analysis also shows a significant gap between best- and worst-case observed conditions for each outage level, showing the relative susceptibility to targeted versus randomized events, and the potential benefits of prioritizing critical substations during restoration.

## IV. Further Analysis of two Methods on Area 5 of the 2000-bus case

In this section, the specific results for Area 5 of the 2000-bus case are further analyzed with the two fragility metrics described in Section II and Section III. This area is the north-central area

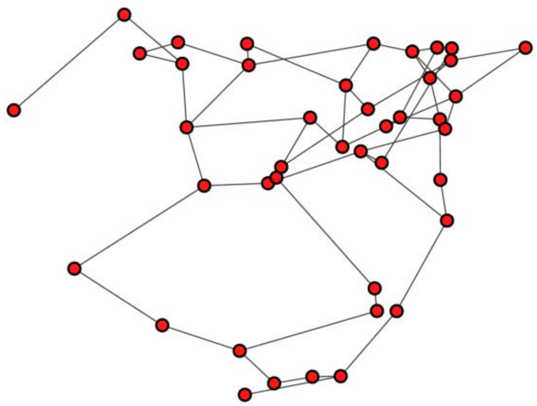

Figure 5. North-Central Region represented as an undirected graph

in Fig. 1, and contains 42 extra-high-voltage substations and 58 extra-high-voltage transmission lines. The main differences conceptually between the connectivity and load delivery metrics stem from their respective assumptions. This area is modeled as an undirected graph, as shown in Fig. 5, for the ATR analysis. The load delivery metric is based on a modeling framework that accounts for generation controls to supply load via lower-voltage lines and support from external areas.

First, we look at the connectivity-based ATR. The exact ATR for all connected subgraphs with $k \leq 5$ is computed using the BDD-based approach as described in Section II. For each $k$, representing the number of transmission line failures, the edges were assumed to fail with probability $p_k = k/\#\mathcal{E}$ . As the computation of exact ATR is computationally infeasible for $k \geq 6$, we approximate the mean ATR, $\overline{\text{ATR}}$, for each $k$ using the $(\epsilon, \delta)$-approximation method of [24] with $\epsilon = 0.1$ and $\delta = 0.05$.

The results from the ATR analysis are summarized in Fig. 6, with $(\epsilon, \delta)$-approximations in agreement with available exact results. This excludes the subgraphs that are disconnected as the ATR for these is assumed zero. The probability distribution of ATR values for a given number of line failures, $k$, is empirically verified to be non-Gaussian. The box plot in Fig. 7 shows the distribution of the ATR values for $k = 1\ to\ 5$. As seen from both Fig. 6 and Fig. 7, the most severe cases (outliers with lowest ATR) are well below the mean ATR for all $k$ from $1\ to\ 5$.

The final two figures zoom in on the individual distributions at a single outage level. For the load delivery method, Fig. 8 shows the distribution of load delivery for 200 sampled scenarios tested with eight EHV substations outaged. This is a non-Gaussian distribution, with a mean near 95% but a rather large lower tail, showing 1-5% of scenarios below 85% of load served, including a cluster that is significantly below the others. Similarly, Fig. 9 shows for the ATR approach a histogram of several hundred thousand k-4 branch outage scenarios on the same network, again demonstrating the non-Gaussian character of the reliability response and a small number of scenarios far from the mean on the tail of the distribution.

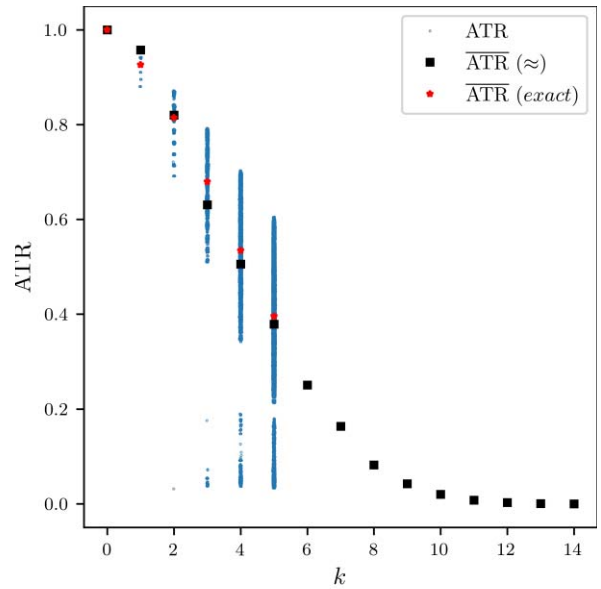


Figure 6. All-terminal reliabilities of subgraphs evaluated using exact BDD-based algorithm and $(\epsilon\ , \delta)$ - approximate algorithm.

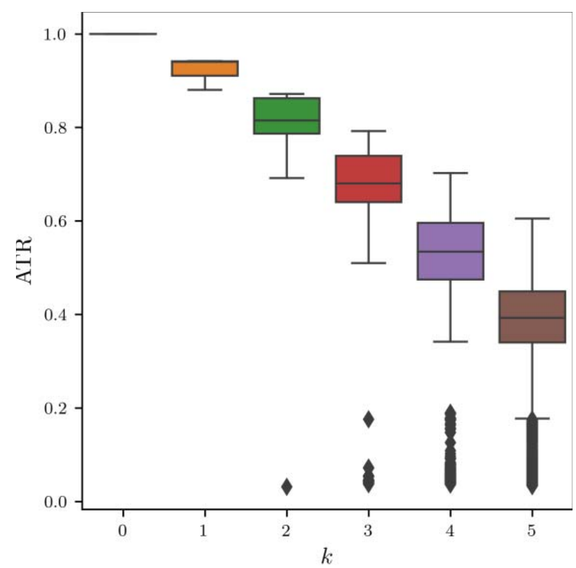


Figure 7. Box plot of exact all-terminal reliabilities of subgraphs for $k = 1\ to\ 5$.

## V. Conclusions and Future work

This paper presents two frameworks that can be used to quantify the fragility and resilience of large electric grids. The ATR method seeks to approximate the true probably-based system reliability metric with a strategic sampling technique. The substation-based dc analysis is a first-order electrical modeling framework that makes best-case operations assumptions to predict how much load can be served. The work in this paper approximates the best, worst, and average cases for each level of system degradation. Future work could seek to improve this level of approximation by additional strategic contingency selection, perhaps proving that a certain set of substations is the worst or best case through a combination of

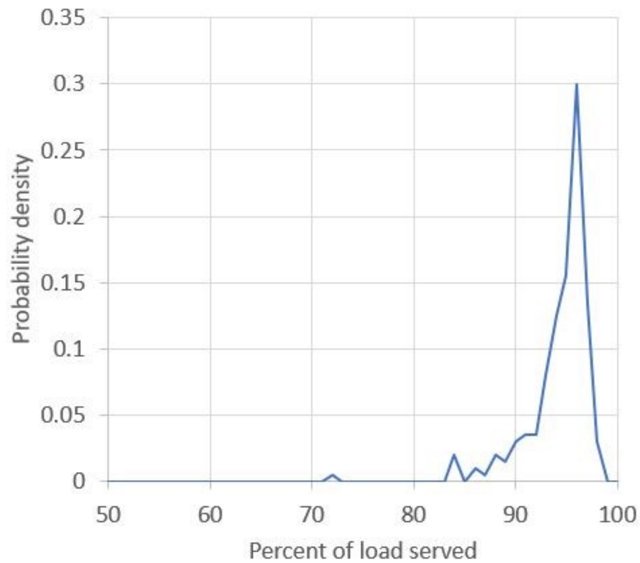


Figure 8. Maximum load delivery distribution for north-central area (green in Fig. 1) under eight substation outages.

topological analysis and optimization. Additional future work may look at persistent substations per bound across percent outages, global failure patterns, and interventions for restorability, both with centralized information and resources, or the more realistic but challenging decentralized approach, as in [25]. Other next steps in this area would also include looking at voltage support aspects of resilience through full ac power flow studies or transient resilience by opening the devices in dynamic simulation.

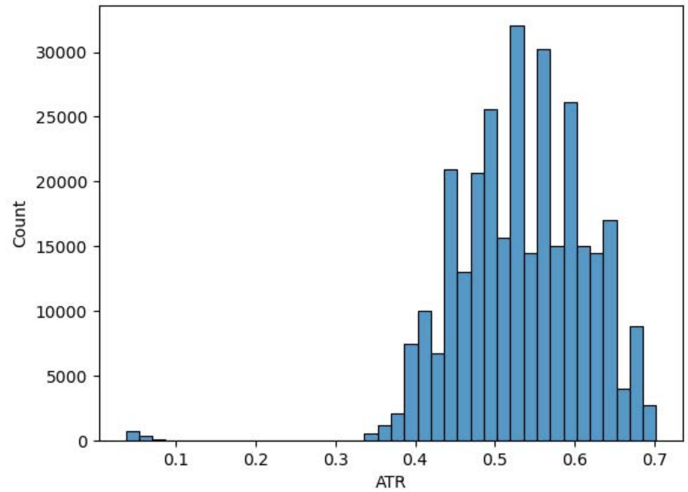


Figure 9. ATR histogram for north-central area (green in Fig. 1) under k-4 branch outages.

## REFERENCES


[1] Z. Bie, Y. Lin, G. Li and F. Li. "Battling the extreme: A study on the power system resilience," *Proceedings of the IEEE*, vol 105, no. 7, pp.1253-1266, Apr. 2017.

[2] M. Shinozuka, et al., "Resilience of integrated power and water systems," Seismic Evaluation and Retrofit of Lifeline Systems, Articles from MCEER's Research Progress and Accomplishments, pp. 65-86, May 2004

[3] M. Panteli, et al., "Power system resilience to extreme weather: fragility modeling, probabilistic impact assessment, and adaptation measures," *IEEE Transactions on Power Systems*, vol. 32, no. 5, pp. 3747-3757, Sept. 2017.

[4] C. Coffrin, et al., "Relaxations of AC Maximal Load Delivery for Severe Contingency Analysis," *IEEE Transactions on Power Systems*, vol. 2, no. 34, pp.1450-1458, March 2019.

[5] M. Kazerooni, H. Zhu and T. J. Overbye, "Mitigation of Geomagnetically Induced Currents Using Corrective Line Switching," in IEEE Transactions on Power Systems, vol. 33, no. 3, pp. 2563-2571, May 2018.

[6] S. Hossain-McKenzie, M. Kazerooni, K. Davis, S. Etigowni and S. Zonouz, "Analytic corrective control selection for online remedial action scheme design in a cyber adversarial environment," in *IET Cyber-Physical Systems: Theory & Applications*, vol. 2, no. 4, pp. 188-197, Dec. 2017.

[7] D. A. Reed, K. C. Kapur and R. D. Christie, "Methodology for Assessing the Resilience of Networked Infrastructure," in *IEEE Systems Journal*, vol. 3, no. 2, pp. 174-180, June 2009.

[8] H. Qi, *et al.*, "A Resilient Real-Time System Design for a Secure and Reconfigurable Power Grid," in *IEEE Transactions on Smart Grid*, vol. 2, no. 4, pp. 770-781, Dec. 2011.

[9] Z. Li, M. Shahidehpour, F. Aminifar, A. Alabdulwahab and Y. Al-Turki, "Networked Microgrids for Enhancing the Power System Resilience," in *Proceedings of the IEEE*, vol. 105, no. 7, pp. 1289-1310, July 2017.

[10] C. Chen, J. Wang, F. Qiu and D. Zhao, "Resilient Distribution System by Microgrids Formation After Natural Disasters," in *IEEE Transactions on Smart Grid*, vol. 7, no. 2, pp. 958-966, March 2016.

[11] D. P. Chassin. and C. Posse. "Evaluating North American electric grid reliability using the Barabási–Albert network model," *Physica A: Statistical Mechanics and its Applications*, vol. 355, no. 2-4, pp. 667-677, Feb. 2005.

[12] Dueñas-Osorio, Leonardo, Kuldeep S. Meel, Roger Paredes, and Moshe Y. Vardi. 2017. "Counting-Based Reliability Estimation for Power-Transmission Grids." In *Proceedings of the Thirty-First AAAI Conference on Artificial Intelligence (AAAI-17)*, 4488–94. San Francisco: Association for the Advancement of Artificial Intelligence.

[13] Paredes, Roger, Leonardo Dueñas-Osorio, Kuldeep S. Meel, and Moshe Y. Vardi. 2019. "Principled Network Reliability Approximation: A Counting-Based Approach." *Reliability Engineering & System Safety* 191 (November): 106472. https://doi.org/10.1016/j.ress.2019.04.025.

[14] A. B. Birchfield, T. Xu, K. M. Gegner, K. S. Shetye and T. J. Overbye, "Grid Structural Characteristics as Validation Criteria for Synthetic Networks," in *IEEE Transactions on Power Systems*, vol. 32, no. 4, pp. 3258-3265, July 2017.

[15] A. B. Birchfield, E. Schweitzer, M. H. Athari, T. Xu, T. J. Overbye, A. Scaglione, and Z. Wang, "A metric-based validation process to assess the realism of synthetic power grids," *Energies*, vol. 10, no. 1233, pp. 1-14, August 2017.

[16] A. B. Birchfield, H. Li, and T. J. Overbye, "Security considerations in transmission planning for creating large synthetic power grids," *Clemson University Power Systems Conference*, Charleston, South Carolina, Sept. 2018.

[17] T. Xu, A. B. Birchfield, and T. J. Overbye, "Modeling, tuning, and validating system dynamics in synthetic electric grids," *IEEE Transactions on Power Systems*, vol. 33, no. 6, pp. 6501-6509, November 2018.

[18] Power flow cases [Online]. Available: electricgrids.engr.tamu.edu

[19] M. O. Ball. "Computational complexity of network reliability analysis: an overview," *IEEE Transactions on Reliability*, vol. 35, no. 3, pp. 230-239, 1986.

[20] G. Hardy, C. Lucet, and N. Limnios. "K-Terminal network reliability measures with Binary Decision Diagrams," *IEEE Transactions on Reliability*, vol. 56, no. 3, pp. 506-515, 2007.

[21] P. Dagum, R. Karp, M. Luby, and S. Ross. "An optimal algorithm for Monte Carlo estimation," *SIAM Journal on Computing*, vol. 29, no. 5, pp. 1484-1496, 2000.

[22] R. Paredes, L. Dueñas-Osorio, K. Meel, and M. Vardi. "Principled network reliability approximation: A counting-based approach," *Reliability Engineering & System Safety*, pp. 191:106472, 2019.

[23] C. Bayer, H. Hoel, E. von Schwerin, and R. Tempone, "On non-asymptotic optimal stopping criteria in Monte Carlo simulations." *SIAM Journal on Scientic Computing*, vol. 36, no. 2, pp. A869-A885, 2014.

[24] M. Huber, "A Bernoulli mean estimate with known relative error distribution," *Random Structures and Algorithms*, vol. 50, no. 2, pp. 173-182, 2017.

[25] H. Talebiyan and L. Duenas-Osorio, "Decentralized Decision Making for the Restoration of Interdependent Networks." *ASCE-ASME Journal of Risk and Uncertainty in Engineering Systems, Part A: Civil Engineering*, vol. 6, no. 2, pp. 04020012, 2020. https://doi.org/10.1061/AJRUA6.0001035

[26] G. Eason, B. Noble, and I. N. Sneddon, "On certain integrals of Lipschitz-Hankel type involving products of Bessel functions," Phil. Trans. Roy. Soc. London, vol. A247, pp. 529–551, April 1955.